Control of the Anisotropic Organization of Nanostructured Silica-Based Hybrid Materials

Bruno Boury,† Frédéric Ben,† Robert J. P. Corriu,*,† Pierre Delord,‡ and Maurizio Nobili‡

Laboratoire de Chimie Moléculaire et Organisation du Solide, UMR 5637, and Groupe de Dynamique des Phases Condensées, UMR 5581, Université Montpellier II, Place E. Bataillon, 34095 Montpellier Cedex 5, France

Received July 19, 2001. Revised Manuscript Received October 5, 2001

This paper concerns the effect of changes in experimental conditions on the micrometric-scale organization observed in hybrid materials obtained from six rigid rod and semi-rigid bis-trialcoxsilylated precursors and one trisilylate after polycondensation at silicon. Different solvents and catalysts have been studied showing that birefringence properties are highly dependent on these parameters. A drastic effect of catalyst is observed especially in the case of basic catalysis, which is more or less capable of inducing a catalytic cleavage of the Si−O−Si bond. For instance, with NaOH either no or very weak birefringence can be observed, but the level of polycondensation at silicon is higher. In summary, the best experimental conditions for micrometric-scale organization are the use of HCl or nucleophilic catalysis (F^-) in THF, DMF, NMF, and toluene.

The chemistry of organic−inorganic hybrid materials is expanding; it opens a wide range of possibilities because it bridges material science, organic, inorganic, and coordination chemistry. We are particularly interested by the nanostructured organic−inorganic materials which are prepared by hydrolytic polycondensation of molecular precursors wherein an organic group is covalently bound to at least two $-SiX_3$ groups (X = OMe, OEt, H, Cl, etc.).[1−7] These precursors lead in a one-step reaction to a solid; the polycondensation at silicon results in a polysiloxane network covalently connected to the organic unit (eq 1 in Scheme 1). The choice of the latter is very broad, permitting the formation of materials with physical and chemical properties. The question about the organization of these materials has to be considered because the placement of the organic spacers between each other can deeply influence the properties of NLO materials,[8,9] luminescent materials,[10−13] thin film with a high or low dielectric constant,[14] or solids such as mesoporous MCM materials.[15,16]

Scheme 1

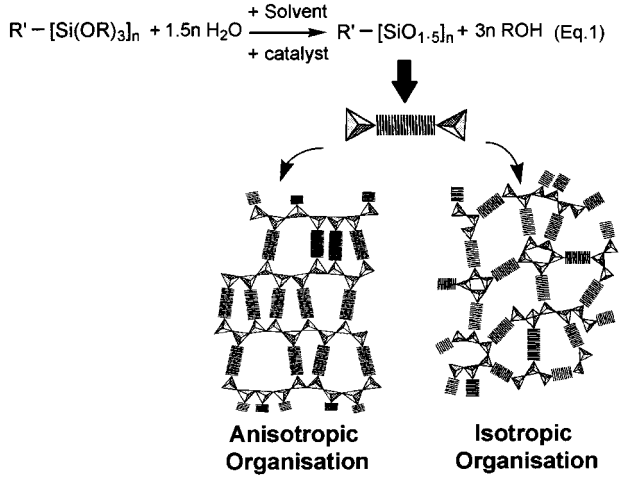

Recently, we proved the possibility of an organization of the precursor units by studying the chemical behavior of the organic group bound to the network.[17,18] In the case of a precursor having a rigid rodlike geometry, this self-organization was checked by X-ray studies[19] and evidenced at a mesoscopic scale by birefringence measurements.[19−21] It is important to point out that

* To whom correspondence should be addressed.
† Laboratoire de Chimie Moléculaire et Organisation du Solide, UMR 5637.
‡ Groupe de Dynamique des Phases Condensées, UMR 5581.

(1) Loy, D. A.; Shea, K. J. *Chem. Rev.* **1995**, *95*, 1431.
(2) Lindner, E.; Scheller, T.; Auer, F.; Mayer, H. A. *Angew. Chem., Int. Ed.* **1999**, *38*, 2154.
(3) Shea, K. J.; Loy, D. A. *Mater. Res. Bull.* **2001**, *5*, 358.
(4) Corriu, R. J. P.; Leclercq, D. *Angew. Chem., Int. Ed. Engl.* **1996**, *35*, 4001.
(5) Corriu, R. J. P.; Leclecq, D. *Angew. Chem., Int. Ed. Engl.* **1996**, *15*, 4001.
(6) Corriu, R. J. P. *Angew. Chem., Int. Ed.* **2000**, *39*, 1376.
(7) Boury, B.; Corriu, R. J. P. In *Supplement Si: The Chemistry of Organic Silicon Compounds*; Rappoport, Z., Apeloig, Y., Eds.; Wiley & Sons: Chichester, 2001; Chapter 10, p 565.
(8) Toussaere, E.; Zyss, J.; Griesmar, P.; Sanchez, C. *Nonlinear Opt.* **1991**, *1*, 349.
(9) Yang, Z.; Xu, C. B.; Dalton, L. R.; Kalluri, S.; Steier, W. H.; Bechtel, J. H. *Chem. Mater.* **1994**, *6*, 1899.
(10) Corriu, R. J. P.; Hesemann, P.; Lanneau, G. *Chem. Commun.* **1996**, 1845.
(11) Shea, K. J.; Loy, D. A.; Webster *Chem. Commun.* **1992**, *114*, 6700.
(12) Franville, A.-C.; Zambon, D.; Mahiou, R. *Chem. Mater.* **2000**, *12*, 428.
(13) Franville, A. C.; Zambon, D.; Mahiou, R.; Chou, S.; Troin, Y.; Cousseins, J. C. *J. Alloys Compd.* **1998**, *275−277*, 831.
(14) Lu, Y.; Fan, H.; Doke, N.; Loy, D.; Assink, R. A.; LaVan, D. A.; Brinker, C. J. *J. Am. Chem. Soc.* **2000**, *122*, 5258.
(15) MacLachlan, M. J.; Asefa, T.; Ozin, G. *Chem. Eur. J.* **2000**, *6*, 14.
(16) Asefa, T.; Yoshina-Ishii, C.; MacLachlan, M. J.; Ozin, G. A. *J. Mater. Chem.* **2000**, *10*, 1751.
(17) Corriu, R. J. P.; Moreau, J. J. E.; Thépot, P.; Wong Chi Man, M.; Chorro, C.; Lèreporte, J. P.; Sauvajol, J. L. *Chem. Mater.* **1994**, *6*, 640.
(18) Corriu, R. J. P.; Moreau, J. J. E.; Thepot, P.; Wong Chi Man, M. *Chem. Mater.* **1996**, *8*, 100.

10.1021/cm011180u CCC: $22.00
Published on Web 01/22/2002

the birefringence observed here cannot be connected to any kind of liquid crystal type previously reported. The precursor $(MeO)_3Si-C\equiv C-C_6H_4-C\equiv C-Si(OMe)_3$ is not a thermotropic liquid crystal while the corresponding xerogel $O_{1.5}Si-C\equiv C-C_6H_4-C\equiv C-SiO_{1.5}$ is birefringent. This phenomenon displays the anisotropic organization of the medium. Moreover, in the case of liquid crystal weak forces such as van der Waals forces are responsible for the formation of anisotropic organization. In contrast, the mesoscopic-scale organization observed here occurs during the cross-linkage of a polysilsesquioxane framework formed of Si−O−Si bonds between nonmesogenic units. We have extended this study to other organic spacers and observed that a rigid rodlike R group is clearly best suited to obtain the anisotrope xerogel, for example, the birefringence observed for R being mono-, bi-, or terphenyl. In contrast, an isotropic no-birefringent medium is obtained with R being an alkyl group.[20]

In this paper we focus on the effect of the experimental conditions of preparation of the xerogels on its anisotropic organization. It has been shown that texture (specific surface area and porosity) of these hybrid materials is at least partially controlled by the kinetic parameters, which govern the polycondensation at silicon. The catalyst and the solvent have been shown to be very effective for the control of the texture.[22,23] In this paper we have studied the effect of both the solvent and different catalysts on the rigid and semirigid precursor **I**−**VII**.

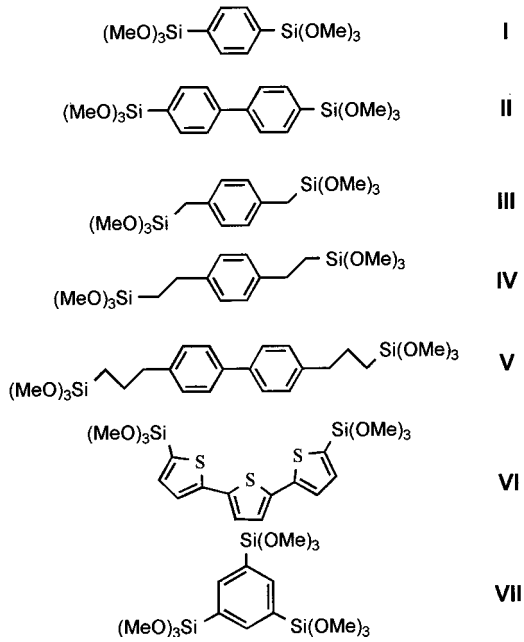

The corresponding hybrid materials $\mathbf{HM_{ncat.}}$ were prepared by sol−gel-type polycondensation, either with different catalysts (Scheme 2) or in different solvents (Scheme 3). In this study, we try to point out what could be the relation between four important characteristics of these solids: the porosity, the level of condensation, the organization at the microscopic level structure, and the birefringence value indicating the isotropic or anisotropic character of the solid.

Scheme 2

PRECURSOR + 3 eq. H_2O + THF as solvent

HCl as catalyst	$\mathbf{HM_{nHCl}}$
nBu_4NF as catalyst	$\mathbf{HM_{nTBAF}}$
NH_4F as catalyst	$\mathbf{HM_{nAF}}$
NH_3 as catalyst	$\mathbf{HM_{nNH3}}$
NaOH as catalyst	$\mathbf{HM_{nNaOH}}$

Scheme 3

II + 3 eq. H_2O + NH_4F as catalyst

in THF	$\mathbf{HM_{IITHF}}$
in Methanol	$\mathbf{HM_{IIMet.}}$
in Toluene	$\mathbf{HM_{IITol.}}$
in Dimethylformamide	$\mathbf{HM_{IIDMF}}$
in Methylformamide	$\mathbf{HM_{IINMF}}$
in Formamide	$\mathbf{HM_{IIForm.}}$

Results

General Procedure. Homogeneous solutions are prepared by mixing in a Shlenk tube at room temperature precursor/solvent/water/catalyst in a 1/10/3/0.01 molar ratio. The stoichiometric amount of water is used for complete hydrolysis of all the Si−OMe groups (3 equiv of water). In some cases, starting mixtures are not homogeneous at first but they become so gradually after 1−5 min. This indicates that the beginning of the reaction leads to species more soluble in polar solvents, with silanol being the most probable to be produced by this reaction. To measure the birefringence, part of the solution is introduced in glass cells similar to those used for analyzing thermotropic liquid crystal; the cells are then analyzed by optical microscopy (Scheme 4).[21] The glasses of the cell are coated with Teflon; other coatings were previously tested like poly(vinyl alcohol) or octadecylsilsesquioane but Teflon was chosen due to its chemical stability.[21] The other part of the solution is gellified in the Schlenk tube and the bulk material formed is used after processing for porosimetry, NMR analyses, and X-ray diffraction analysis.

Effect of the Catalyst. Four catalysts were used to promote the gelation of the solution. The amount of catalyst was adjusted to avoid too short or too long gelation times that are not compatible with manipulation in cells. Therefore, the same molar ratio of catalyst is not always used and consequently gelation time of the solutions are different but cannot be compared and interpreted directly. With this idea, the effect of the catalyst's concentration could not be checked, although it is certainly a determining parameter.

(19) Boury, B.; Corriu, R. J. P.; Delord, P.; Le Strat, V. *J. Non-Cryst. Solids* **2000**, *265*, 41.
(20) Ben, F.; Boury, B.; Corriu, R. J. P.; Le Strat, V. *Chem. Mater.* **2000**, *12*, 3249.
(21) Boury, B.; Corriu, R. J. P.; Delord, P.; Nobili, M.; Le Strat, V. *Angew. Chem., Int. Ed.* **1999**, *38*, 3172.
(22) Cerveau, G.; Corriu, R. J. P.; Framery, E. *J. Mater. Chem.* **2000**, *10*, 1617.
(23) Cerveau, G.; Corriu, R. J. P.; Lepeytre, C. *J. Mater. Chem.* **1999**, *9*, 1149.

Scheme 4

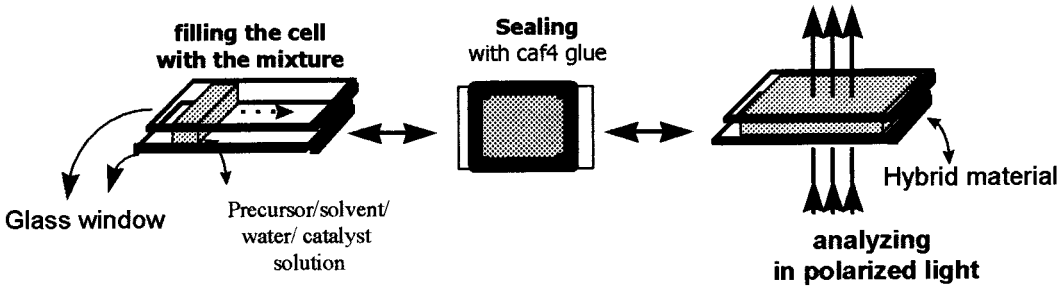

In all cases, the initial solutions were completely dark when analyzed by polarized optical microscopy; this observation is characteristic of an isotropic medium. When they form, all the gels are transparent, allowing a clear observation and measurement of the characteristics by optical microscopy. Aging of the wet gels leads to the formation of cracks due to syneresis and hydrodynamic processes, classical phenomena in sol−gel-type processes of silica-based materials.[24] These phenomena result from first the loss of 6 equiv of methanol for each equivalent of monomer and second to the presence of solvent. The large volume loss upon evaporation of solvent and byproducts leads to the shrinkage of the gel and to cracking of the initial monolith that forms at the gel point. For **HM$_{IHCl}$**, birefringent pieces of gel result from the cracking of the gel. Pictures of cells clearly show the presence of bright pieces of solids separated by dark zones corresponding to the cracks; examples are given in Pictures I and II. After more than a month, the solvent was evaporated by slow diffusion and the materials can be considered as xerogels. Birefringence's values are given in Table 1; they are average values and it is important to note that these values remain unchanged even several months after the initial measurement. The same type of observation can be made for gels and xerogels prepared with F^- catalyst: **HM$_{ITBAF}$** and **HM$_{IAF}$**.

Picture I of **MH$_{IIHCl}$** by microscopy in polarised light

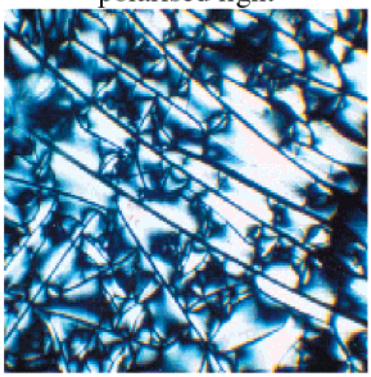

Picture II of **MH$_{IIAF}$** by microscopy in polarised light

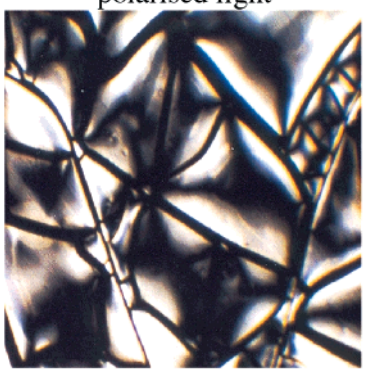

Table 1. Birefringence and Specific Surface Area of Xerogels HM$_{ncat.}$ Prepared in THF as the Solvent at 25 °C

xerogel	catalyst (% per mol)	gelation time (min)	SSA[a] ($m^2\ g^{-1}$)	∅ pores	Δn (10^{-3})
HM$_{IAF}$	NH_4F (1%)	3	1220	5−20[b]	2
HM$_{INH3}$	NH_3 (4%)	30	1050	5−20[b]	<0.1
HM$_{INaOH}$	NaOH (4%)	70	980	5−20 + 30−40[c]	0
HM$_{IHCl}$	HCl (3%)	10	580	5−20[b]	2
HM$_{ITBAF}$	TBAF (1%)	1	1460	30−40[d]	<0.1
HM$_{IIAF}$	NH_4F (1%)	45	1050	5−20[b]	3
HM$_{IINH3}$	NH_4OH (4%)	90	870	5−20[b]	2
HM$_{IINaOH}$	NaOH (4%)	30	1130	5−20[b]	0
HM$_{IIHCl}$	HCl (3%)	10	710	5−20[b]	4
HM$_{IITBAF}$	TBAF	2	1490	5−20[b]	2.5
HM$_{IIINaOH}$	NaOH (4%)	180	540		2
HM$_{IIIHCl}$	HCl (3%)	5	<10		2
HM$_{IVNaOH}$	NaOH (4%)	360	300		0
HM$_{IVHCl}$	HCl (3%)	6	<10		1.5
HM$_{VNaOH}$	NaOH (4%)	360	<10		0
HM$_{VHCl}$	HCl (3%)	5	<10		8
HM$_{VINaOH}$	NaOH (4%)	10			<0.1
HM$_{VIHCl}$	HCl (3%)	6			10
HM$_{VIINaOH}$	NaOH (4%)	1			0.3−0
HM$_{VIIHCl}$	HCl (3%)	1			1

[a] Specific surface area. Care must be taken when considering these values since some of these solids are microporous and specific surface determined by the BET method is not very accurate in this case. [b] Mainly microporous. [c] Micro- and mesoprous. [c] Only mesoporous.

When the catalyst is NH_3, birefringence is observed for **HM$_{INH3}$** and **HM$_{IINH3}$** but is always lower than the birefringence of the corresponding materials prepared with HCl or F^- as catalyst (Picture III).

With NaOH as catalyst gelation occurs and cracking leads to pieces of gel that are either not birefringent (**HM$_{n\text{NaOH}}$**, n = **I**, **II**, **IV**, **V**) or their birefringence is much lower and limited to very tiny zones inside the chunks of the material like for **HM$_{VIINaOH}$**. Because both the solid and the cracks are isotropic regions, the difference between them is difficult to distinguish in polarized light (Picture IV). The case of **HM$_{IIINaOH}$** is the only one for which xerogel prepared with HCl or NaOH have the same birefringent value ($\Delta n = 2 \times 10^{-3}$).

(24) Brinker, C. J.; Scherer, G. W. *Sol−Gel Science*; Academic Press: Boston, 1990.

Picture III of $\mathbf{MH_{IINH3}}$

by microscopy in polarised light

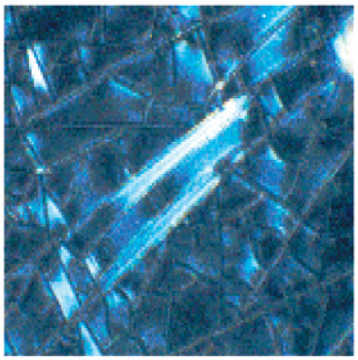

Picture IV of $\mathbf{MH_{VIINaOH}}$

by microscopy in polarised light (the picture is highlighted)

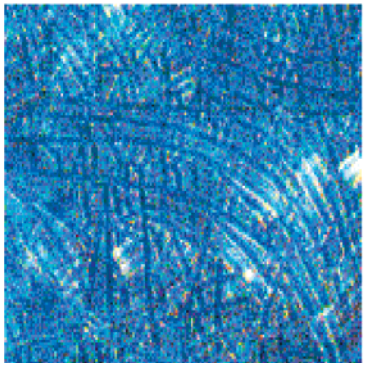

The catalyst also has an effect on both the cracking of the gel and the shape of the pieces; these phenomena are purely qualitative. For example, periodical cracking is frequently observed with HCl or F^- (Picture V). In

Picture V

Example of periodical cracking observed for $\mathbf{MH_{IIAF}}$

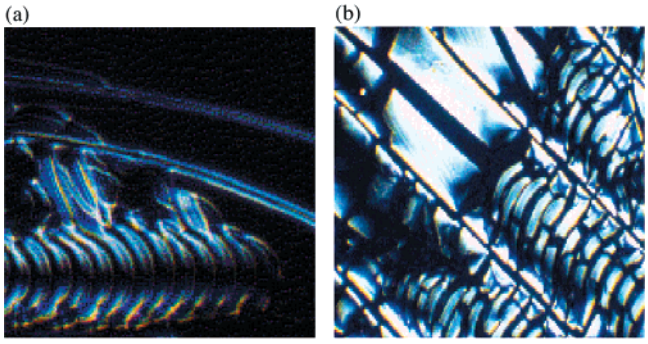

basic conditions each piece of xerogel has a different shape (see, for example, Picture IV). However, this is beyond any interpretation today.

Powder X-ray diffraction analysis of these materials was performed to obtain information on the organization in microscopic order, as previously reported for $O_{1.5}Si-CC-C_6H_4-CC-SiO_{1.5}$ xerogels.[19] We focus on xerogels prepared from **I** or **II**, using HCl or NaOH as the catalyst (Figure 1) and exhibiting very different values of birefringence. Like for other nanostructured hybrid materials,[7] a broad signal is generally observed at 1.7–1.9 $Å^{-1}$ for all the solids prepared in this study; it is

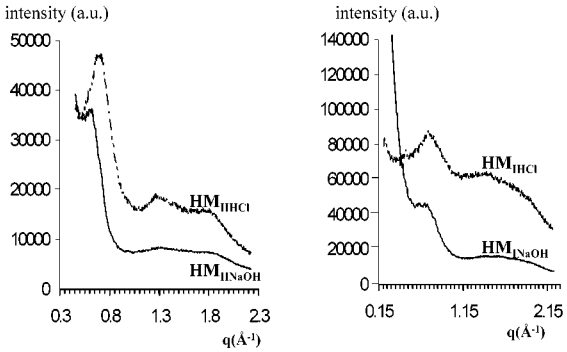

Figure 1. Diffractogram of a X-ray diffraction powder analysis of $\mathbf{HM_{INaOH}}$, $\mathbf{HM_{IHCl}}$, $\mathbf{HM_{IINaOH}}$, and $\mathbf{HM_{IIHCl}}$.

attributed to the contribution of the Si–O–Si units by comparison with SiO_2 xerogels prepared with TMOS. For the hybrid, two other broad signals are observed around 0.7–0.6 and 1.3 $Å^{-1}$. Actually, for both **I** and **II**, the X-ray diffraction pattern of the corresponding solids prepared in acidic or basic conditions are broadly similar; however, we can observe three main differences. First, a variation of the intensity at low q value can be ascribed to the difference of porosity between the xerogels. As will be seen below, a higher porosity is observed for $\mathbf{HM_{INaOH}}$ and $\mathbf{HM_{IINaOH}}$ than for $\mathbf{HM_{IHCl}}$ and $\mathbf{HM_{IIHCl}}$; this can explain the higher intensity located at small-angle q vectors. Second, a difference in location of the peaks is obvious; this is especially clear in the case of precursor **II**: 0.7 $Å^{-1}$ for $\mathbf{HM_{IIHCl}}$ and 0.55 $Å^{-1}$ for $\mathbf{HM_{INaOH}}$. Finally, the relative intensity of this peak compared to the signal at 1.7 $Å^{-1}$ is not equal for solids prepared in acidic and basic conditions. The differences in birefringence values observed above between solids prepared with different catalysts agree with the differences observed by microscopy in polarized light.

Porosimetry measurements were also performed on the materials prepared in bulk quantity (in a Schlenk tube) to have an idea of the specific surface area and the characteristics of the porosity (Table 1). Previous studies have pointed out the role of the catalyst on the porosity of these materials in relation to the nature of the organic moiety.[22,23] As a general trend, we found here that xerogels prepared with NaOH or NH_4F as catalysts always exhibit a higher specific surface area than xerogels prepared with HCl. For all the xerogels, similar isotherms are obtained and are typical of highly microporous materials, a broad pore size distribution being observed with pore size in the range of $5 < ∅ < 50$ Å. Only in the case of NaOH as the catalyst and for **I**, a high percentage of mesopores (∅ 40 Å) are observed (Figure 2). The absence of birefringence of xerogels prepared with NaOH, $\mathbf{HM_{IINaOH}}$ for example, cannot be related to a very high or very low specific surface area or to the presence of a high level of micropores. Indeed, microporous materials with higher ($\mathbf{HM_{IITBAF}}$) and lower ($\mathbf{HM_{IIHCL}}$) specific surface area are birefringent. The same observation is true for precursor **I**. So far, we are not able to draw any relationship between the porosity of these solids and their birefringence.

When comparing the levels of condensation of these solids by ^{29}Si NMR spectroscopy, we found that it is generally high as indicated by the presence of T^1 [C–*Si*$(OR)_2$–(O–Si)], T^2 [C–*Si*(OR)–$(O–Si)_2$], and T^3

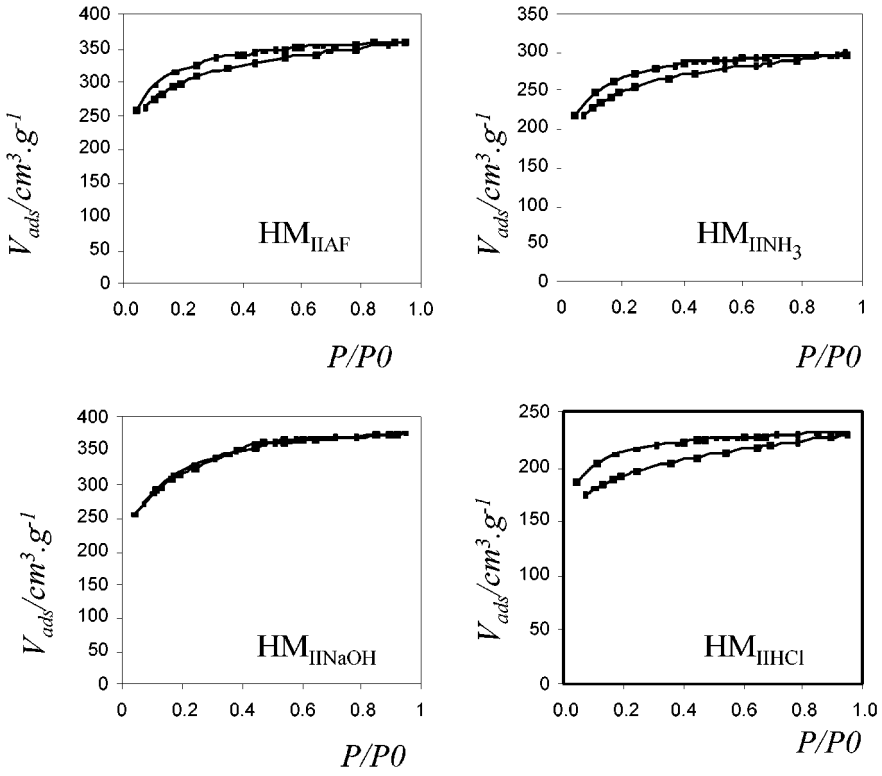

Figure 2. Isotherm plot of $\mathbf{HM_{INaOH}}$, $\mathbf{HM_{IHCl}}$, $\mathbf{HM_{IAF}}$, and $\mathbf{HM_{INH3}}$.

Table 2. CP MAS ^{29}Si NMR Data of Xerogels $\mathbf{HM_{ncat.}}$ Prepared in THF as Solvent at 25 °C

	polycondensation level			
xerogel	T^1	T^2	T^3	total
	−62 ppm	−70 ppm	−78 ppm	
$\mathbf{HM_{IAF}}$	21	58	21	66
$\mathbf{HM_{INH3}}$	31	46	23	64
$\mathbf{HM_{INaOH}}$	20	47	32	70
$\mathbf{HM_{IHCl}}$	25	60	13	62
$\mathbf{HM_{ITBAF}}$	26	50	24	66
	−61 ppm	−70 ppm	−78 ppm	
$\mathbf{HM_{IIAF}}$	14	41	44	76
$\mathbf{HM_{IINH3}}$	30	40	28	66
$\mathbf{HM_{IINaOH}}$	14	28	57	81
$\mathbf{HM_{IIHCl}}$	27	59	13	61
$\mathbf{HM_{IITBAF}}$	14	52	34	73
	−54 ppm	−61 ppm	−69 ppm	
$\mathbf{HM_{IIINaOH}}$	20	43	37	73
$\mathbf{HM_{IIIHCl}}$[a]	29	27	17	44
	−50 ppm	−59 ppm	−67 ppm	
$\mathbf{HM_{IVNaOH}}$	6	41	53	81
$\mathbf{HM_{IVHCl}}$	21	52	27	69
	−57 ppm	−65 ppm	−76 ppm	
$\mathbf{HM_{VNaOH}}$	8	36	56	83
$\mathbf{HM_{VHCl}}$	9	64	27	73
	−65 ppm	−73 ppm	−80 ppm	
$\mathbf{HM_{VINaOH}}$	14	40	46	78
$\mathbf{HM_{VIHCl}}$	15	49	36	74
	−62 ppm	−70 ppm	−78 ppm	
$\mathbf{HM_{VIINaOH}}$	34	58	8	58
$\mathbf{HM_{VIIHCl}}$	46	51	3	52

[a] Signal at −19 ppm is present in this case and corresponds to T^0 units.

[C−*Si*(O−Si)$_3$] signals (see Table 2).[25] However, it is not the highest level of polycondensation possible since this would lead to the presence of only T^3 signals. CP MAS spectroscopy is generally not quantitative; however, when compared with single-pulse experiments (that allow a quantitative determination), no significant variation in relative peak intensity was observed in the case of such alkylene or arylene nanostructured solids.[23,26] Moreover, since materials of the same precursor are compared, it can be assumed that relative peak intensity can be used to show a variation of the level of condensation between them. The level of condensation was determined according to the general equation LC = 0.66 [0.5(T^1area) + 1.0(T^2area) + 1.5(T^3area)]. We found that both the highest level of condensation and the highest level of T^3 units are always both observed for $\mathbf{HM_{nNaOH}}$. In contrast, the xerogels $\mathbf{HM_{nHCl}}$ prepared with HCl have the lowest level of condensation with T^1 and mainly T^2 units (an example is given in Figure 3). An intermediate situation is observed for $\mathbf{HM_{nAF}}$ and $\mathbf{HM_{nTBAF}}$, the level of condensation and the proportion of $T^1/T^2/T^3$ units being within those of xerogels prepared with HCl and NaOH. Finally, NMR data for xerogel $\mathbf{HM_{nNH3}}$ have a closer resemblance to those of xerogels prepared with F^- as the catalyst than to those prepared with NaOH. This is confirmation of the great difference between these two catalysts.

These results indicate a possible relationship between the level of condensation of the solid and its birefringence. The drastic difference of birefringence values between xerogels cannot be directly and only explained by a difference in the average level of condensation. However, this result reflects a difference in the Si−O−Si framework.

Solvent Effect. To investigate the effect of the solvent on this process, precursor **II** was polycondensed

(25) Marsmann, H., Dielh, P., Fluck, E., Kosfeld, R., Eds. *Basic Principles and Progress in NMR Spectroscopy*; Springer-Verlag: Berlin, 1981; Vol. 17, p 65.

(26) Oviatt, H. W.; Shea, K. J.; Small, J. H. *Chem. Mater.* **1993**, *5*, 943.

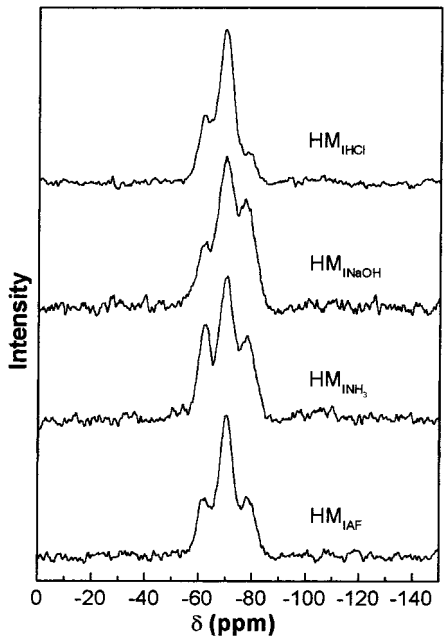

Figure 3. ^{29}Si NMR CP MAS analysis of **HM$_{Icat.}$**, with cat. (catalyst) being HCl, NaOH, NH_4OH, and NH_4F.

in various solvents with 3 equiv of water and using NH_4F as the catalyst (1% molar ratio). The solvents were chosen according to their different polarities (μ), dielectric constants (ϵ), and protic character: methanol, THF, toluene, dimethylformamide, *N*-methylformamide, and formamide (Table 3). Formamide was used as drying control chemical additives for silica gels,[27−30] and in the case of nanostructured materials formamide was successfully used to avoid cracking and to obtain clear monolith.[1]

Here, all the initial solutions were completely dark when analyzed by microscopy in polarized light characterizing an isotropic medium. Very different gelation times of the solution were observed, revealing how important the intervention of the solvent in this process can be. Basic or polar solvents lead to shorter gelation times. All the gels were found to be transparent with the exception of the gel prepared in methanol **HM$_{IIMeOH}$** (Picture VI**)** for which a very white opaque solid is formed, preventing the study of the birefringence. This is certainly due to a light diffusion phenomenon and indicates that particles with a size higher than the wavelength of the light are formed.

In all cases, syneresis and cracking of the gel were observed with the exception of **HM$_{IIForm}$**. In agreement with the property of this solvent as a drying chemical controlling additive, a transparent pasty mixture is formed from which evaporation of the formamide is extremely slow and cracking is avoided (another possibility to obtain crack-free solids could be to cast them into thin film[31]). In the other cases, an observation of the aging process indicates that the birefringence initially appears as a birefringent zone on each side of

Picture VI
Observation of **MH$_{IIMeOH}$** by microscopy in polarised light

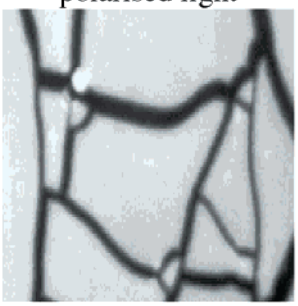

the cracks that cut through the gels; the widths of these zones vary from 10 to 50 μm and depend on the nature of the solvent (compare Picture II of **HM$_{IIAF}$** prepared in THF and Picture VII of **HM$_{IIDMF}$**). Birefringence

Picture VII
Observation of **MH$_{IIDMF}$** by microscopy in polarised light

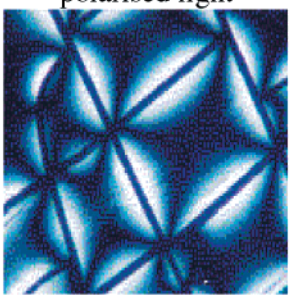

inside the chunks of gel is observed progressively when aging and evaporation of the solvent along with additional cracking lead to smaller pieces of solid (Scheme 5). The effect of the nature of the solvent on the birefringence is clear and important (Table 3). For instance, the value for materials prepared in DMF is 3 times stronger than for solids prepared in toluene.

The nature of the solvent, just like the nature of the catalyst, is known to modify the porosity of this type of $O_{1.5}Si-R-SiO_{1.5}$ solids;[23] indeed, we found different specific surface areas and different pore size distributions for all these birefringent solids prepared in different solvents (Table 3). As could be expected from previous results, the formamide leads to a microporous solid with very low specific surface area. Other solids are either microporous with a various percentage of mesopores (in MeOH, toluene, THF, or DMFH) or mainly mesoporous solids with a very broad pore size distribution $5 < \varnothing < 120$ Å like for **HM$_{IINMF}$**.

The effect of solvent is shown by the characteristics of the Si−O−Si framework characterized by the level of condensation and the $T^1/T^2/T^3$ signals' intensity. However, the variation of the level of polycondensation of these solids is rather low (7−8%) and cannot be clearly related to a variation of the birefringence. It is interesting to note that although the gelation times are

(27) Adachi, T.; Sakka, S. *J. Mater. Sci.* **1987**, *22*, 4407.
(28) Adachi, T.; Sakka, S. *J. Non-Cryst. Solids* **1988**, *99*, 118.
(29) Hench, L. L. *Science of Ceramic Chemical Processing*; Wiley: New York, 1986.
(30) Wallace, S.; Hench, L. L. In *Better Ceramics Through Chemistry, Mater. Res. Soc. Symp. Proc.*; Brinker, C. J., Clark, D. E., Ulrich, D. R., Eds.; Material Research Society: New York, 1984; Vol. 32, p 47.
(31) Brinker, C. J.; Raman, N. K.; Logan, M. N.; Sehgal, R.; Assink, R. A.; Hua, D. W.; Ward, T. L. In *ACS Symposium Series—Inorganic and Organometallic Polymers II*; American Chemical Society: Washington, DC, 1994; Vol. 572, p 104.

Table 3. Characteristics of the Birefringence and Specific Surface Area of Xerogels of Precursor II Prepared in Various Solvents at 25 °C with NH_4F as the Catalyst

xerogel	solvent	μ^c (D)	ϵ^c (20 °C)	time[a] (min)	SSA[b] ($m^2\ g^{-1}$)	∅ pores	Δn (10^{-3})	polycondensation level			
								T^1	T^2	T^3	total
HM_{IIDMF}	DMF	3.82	36.7	1	1720	5−40[d]	4.5	10	48	42	77
HM_{IITHF}	THF	1.63	7.6	45	1270	5−20[d]	3	14	41	44	76
HM_{IINMF}	NMF	3.83	182	0.4	1470	5−120[e]	2	17	54	29	71
$HM_{IITol.}$	toluene	0.36	2.4	1800	1050	5−30[d]	1.5	16	55	29	71
HM_{IIMeOH}	MeOH	1.70	32.7	2	960	5−40[d]		15	51	34	73
$HM_{IIForm.}$	formamide	3.73	109	15	360	5−120[e]		27	47	26	66

[a] Gelation time. [b] Specific surface area. [c] Handbook of chemistry, 60th ed. [d] Mainly microporous. [e] Micro- and mesoporous.

Scheme 5

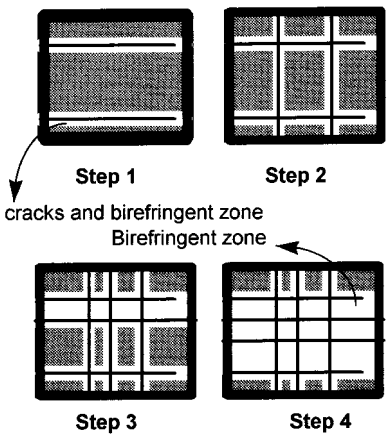

Formation of cracks and birefringent zone during the ageing and syneresis process

very dependent on the nature of the solvent, finally the level of condensation for the gels is more or less the same. It stresses the question of the structure of the colloids and the level of condensation at the gel point.

Discussion

The sol−gel process is a polymerization that allows adjustments of (a) the morphology, (b) the porosity, and (c) the organization of the materials, although a precise comprehension of these processes has not yet been achieved. For the nanostructured solids studied here, the overall process of formation of these materials is deeply controlled by the kinetics of the chemical reaction and the nature of the precursor; in other words, they are kinetically controlled solids.[7] Concerning the organization, the nature of the R group was already reported as a key parameter for the formation of an anisotropic organization in these hybrid materials.[20] We have now proven that the nature of the catalyst and of the solvent used for gelation is also two deciding kinetic parameters for this phenomenon. However, they do not have the same importance; the solvent can introduce variations of the birefringence's intensity whereas the catalyst can lead either to a birefringent or a nonbirefringent material. On the basis of these results, it can be assumed that, for a given precursor, the birefringence depends on a set of parameters that governs the chemistry of the process: nature and concentration of the different compounds (precursor, solvent, catalyst, water), temperature, and so forth.

From a general staring point, the birefringence phenomenon shows the anisotropic organization of the solid at the mesoscopic level. When it is observed, the birefringence always appears first on the edges of the cracks that cut through the wet gels. This indicates that the anisotropic organization of the solid at the mesoscopic level is closely linked to this cracking process and the anisotropic stress developed along the axis of propagation of the cracks. However, besides this mesoscopic process, it is necessary to consider this phenomena at the molecular level and to consider the species of the sol: oligomers, polymers, and colloids. These species and their structures are the result of a set of chemical reactions and their kinetics.

The effect of the solvent on the birefringence is obvious. At the microscopic level, the solvent may enhance or limit an autoassociation of precursor units during the formation of oligomer, polymer, and colloids. This depends on the balance of the interaction between the different species and the solvent. At the mesoscopic level, the intensity of the anisotropic stress produced by the cracking is related to the physicochemical property of the solvent like its viscosity, dipole moment, dielectric constant, and surface tension; all of the above are related to the formation of the cracks, which also result in the formation of surfaces.[7]

Concerning the effect of the catalyst, it is clear that its nature can deeply modify the birefringence of the material. While NaOH as a catalyst generally leads to a nonbirefringent solid, all the other catalysts lead to more or less birefringent solids. The difference of birefringence is corroborated by the difference of organization at the microscopic level as illustrated by the X-ray diffraction analyses.

When looking at other characteristics of the solids, we did not find any clear relationship between the birefringence and the porosity of the materials. Consequently, it can be assumed that these characteristics of the materials result either from different processes or occur at different stages during the formation of the solid.

The effect of the catalyst on the birefringence has to be considered at the molecular level. First, it is well-known that the cleavage of Si−O−Si bonds can occur with NaOH.[32] This chemical cleavage may lead to a reorganization of the Si−O−Si network in an isotropic organization.[33]

On the other hand, birefringence is observed on the edges of the cracks and suggests that it results from the ability of the material to relax the stress orthogonal to the cracks. Such a process leads to the orientation of the organic moieties along the residual stress parallel to the cracks. When one looks at the NMR data, the

(32) Bazan, V.; Chvalovsky, J. *Chemistry of organosilicon compounds*; Academic Press Inc.: New York, 1965.
(33) Cerveau, G.; Corriu, R. J. P.; Framery, E. *C. R. Acad. Sci. Paris, t.2, Sér. IIc* **2001**, *4*, 79.

level of polycondensation and of T^3 units is higher for $\mathbf{HM}_{n\mathbf{NaOH}}$; these cases correspond to structures that are more cross-linked than for $\mathbf{HM}_{n\mathbf{HCl}}$ or $\mathbf{HM}_{n\mathbf{AF}}$. For the latter cases, a low level of polycondensation can allow the species (oligomer, polymer, clusters, etc.) the possibility of an autoassociation, while a more cross-linked 3D architecture may prevent it. At another level, the distortion of the materials upon cracking and the orientation of the substructure by relaxation along the crack are more possible for the less cross-linked structure and more limited for a 3D architecture.

Finally, we note that ammonia and sodium hydroxide give different results. The clear difference of birefringence between $\mathbf{HM}_{n\mathbf{NH3}}$ or $\mathbf{HM}_{n\mathbf{NaOH}}$ demonstrates that these two catalysts cannot be used equally as "basic" catalysts. These observations suggest that NH_3 could act more as a nucleophile than as a base because of the low polarity of the medium and the low basic property of ammonia. Additionally, HN_3 may lead to a Si−O cleavage in a milder and slower way than NaOH.

Conclusion

These results evidence the drastic importance induced by experimental parameters on the mesoscopic organization of the solids. However, we should not only consider this aspect. The organization of the solid is also controlled by the reorganization occurring during its aging. As previously observed, the birefringence (mesocopic organization) appears after the gelation point during aging when formation of the cracks occurs.

From the sum of the preceding results, it may be proposed that the anisotropic organization evidenced by the birefringence arises from the synergy between different phenomena: the autoassociation of the organic group during the hydrolysis/polycondensation, the formation of the Si−O−Si bonds that bring the precursor units closer together, and finally the cracking of the gel that produces an anisotrope stress during its aging.

Experimental Section

Preparation of the cell has been reported previously (30−40 μm of thickness, 3 × 3 cm L, Teflon was chosen as the coating for the glass due to its chemical stability.[20] The gelation time of the solution in the cell is estimated by the absence of any induced hydrodynamic movement.

Optical properties of the material were observed with a Laborlux12POLS polarizing microscope. Photographs were taken using a Leica wild MPS28 camera). The birefringence is obtained from the expression $\Delta l = \Delta n d$, where Δl is the optical path difference and d is the cell thickness. Δl is measured by a Berek compensator.

The birefringence of the material is illustrated by the presence of dark and bright regions under crossed polarizers in polarized light. They indicate a variation of the orientation of the optical axis in the material apparently following the edges of the chunks.

^{29}Si NMR spectra were recorded on a AM300 at 59.620 MHz, a 10-s acquisition time, 2-ms contact time, 7400 scans, and 5000-Hz rotating speed were used. Chemical shifts are indicated in ppm regarding TMS. Porosimetry measurements were performed either on a Micromeritics Gemini III or a Micromeritics ASAP 2010 porosimeter using N_2 at 77 K as the adsorbent. Samples were outgassed at 100 °C under a 0.1 mmHg vacuum before analysis. The equilibrium time was set to 5 s. The specific area was calculated using the BET equation. The mesoporous distribution was calculated by B.J.H's method by applying Harkins and Jura's equation. The microporous distribution was obtained using the Horvath−Kawazoe method with the Saito−Foley equation.

The preparation of precursors **I**,[34] **II**,[34] **III**,[35] **VI**,[17] and **VII**[34] has been previously reported. Precursor **IV** was purchased from ABCR and distilled before reaction.

Preparation of 4,4′-Bis(prop-1-enyl)biphenyl. An excess of *n*-propylmagnesium bromide (200 mmol, 4 equiv) was added dropwise to an ice-cooled and stirred mixture of 4,4′-dibromobiphenyl (15.6 g, 50 mmol) and (dppp)$NiCl_2$ (270 mg, 0.5 mmol) in dry THF (100 mL). The cooling bath was removed and the mixture was refluxed overnight. It was then carefully quenched by HCl aqueous solution (500 mL, pH = 1). An aqueous layer was extracted with ether (2 × 200 mL), and the combined organic layer was washed with H_2O (100 mL) and dried ($MgSO_4$). Recrystallization from ^{i}PrOH/$CHCl_3$ (1/1) gave 7.4 g as a white powder. Yield: 65%. ^{1}H NMR ($CDCl_3$, δ): 3.47 (d, 4H), 5.16 (m, 4H), 6.03 (m, 2H), 7.30 (d, 4H), 7.56 (d, 4H) ppm. ^{13}C NMR ($CDCl_3$, δ): 40.3, 116.3, 127.5, 129.4, 137.8, 139.3, 139.4 ppm.

Preparation of 4,4′-Bis(trimethoxysilylpropyl)biphenyl (5). A mixture of 4,4′-bis(prop-1-enyl)biphenyl (12.33 g, 53 mmol) and H_2PtCl_6 (20 mg, 5 mmol) in dry hexane (150 mL) was stirred for 30 min. Then, trichlorosilane (25 mL, 253 mmol) was added dropwise (15 min) and the mixture was stirred overnight. Solvent and excess $HSiCl_3$ were evaporated off. The resulting product was dissolved in hexane (100 mL) and added to a solution of methanol (65 mL, 1.65 mol) and triethylamine (230 mL, 1.65 mol). The mixture was stirred overnight. After filtration of the salt and concentration under reduced pressure, distillation (180 °C, 0.05 mmHg) gave 6.155 g of a cream color oil. Yield: 30%. ^{1}H NMR ($CDCl_3$, δ): 0.77 (m, 4H), 1.81 (m, 4H), 2.73 (t, 4H), 3.60 (s, 17H), 7.28 (d, 4H), 7.55 (d, 4H) ppm. ^{13}C NMR ($CDCl_3$, δ): 9.38, 25.03, 39.18, 50.94, 127.40, 129.33, 139.05, 141.47 ppm. ^{29}Si NMR ($CDCl_3$, δ): −41.50 ppm.

General Procedure for the Synthesis of the Xerogels. In a Schlenk flask under nitrogen, precursors and THF were mixed and stirred vigorously. The catalyst, either ammonium fluoride NH_4F (0.19, 0.37, or 0.74 M in H_2O) or ammonia NH_3 (0.74 M in H_2O) or hydrochloric acid HCl (0.55 M in H_2O) or sodium hydroxide NaOH (0.74 M in H_2O) or tetrabutylammonium fluoride TBAF (1 M in THF), was added, and the mixture was stirred for an additional 2 min. The stirring was then stopped to allow the gelation to occur in a steady solution gelation. At first, a monolith is obtained and occupies the same volume as the initial solution. The gel was allowed to stand 1 week for aging and then was crushed, washed with acetone (20 mL), ethanol (20 mL), and diethyl ether (20 mL), and finally dried for 24 h at 100 °C under vacuum (0.1 mmHg). Yields of preparation are sometime higher than 100% due to the presence of a residual amount of solvent and Si−OR (R = H or Me) group. The same experimental procedure is used for preparing all the xerogels. Gelation times are given in Table 1 and ^{29}Si NMR CP-MAS data are given in Table 2.

Xerogel $\boldsymbol{HM_{IAF}}$**.** The mixture for gelation was made with 1.22 g (3.8 mmol) of **I**, 3.8 × 10^{-2} mmol of NH_4F, 11.4 mmol of water, and 1.27 mL of THF. Gelation time was 3 min. Mass of xerogel: 0.762 g. Yield: 110%.

Xerogel $\boldsymbol{HM_{INH3}}$**.** The mixture for gelation was made with 1.45 g (4.6 mmol) of **I**, 18.1 × 10^{-2} mmol of NH_4OH, 13.5 mmol of water, and 1.52 mL of THF. Gelation time was 30 min. Mass of xerogel: 0.784 g. Yield: 95%.

Xerogel $\boldsymbol{HM_{INaOH}}$**.** The mixture for gelation was made with 1.52 g (4.7 mmol) of **I**, 18.8 × 10^{-2} mmol of NaOH, 14.1 mmol of water, and 1.59 mL of THF. Gelation time was 70 min. Mass of xerogel: 0.871 g. Yield: 102%.

Xerogel $\boldsymbol{HM_{IHCl}}$**.** The mixture for gelation was made with 1.45 g (4.6 mmol) of **I**, 13.5 × 10^{-2} mmol of HCl, 13.5 mmol of water, and 1.52 mL of THF. Mass of xerogel: 0.890 g. Yield: 108%.

(34) Corriu, R. J. P.; Moreau, J. J. E.; Thépot, P.; Wong Chi Man, M. *Chem. Mater.* **1992**, *4*, 1217.

(35) Motevalli, M.; LiOu, D.; Sullivan, A. C.; Carr, S. W. *J. Organomet. Chem.* **1978**, *150*, 27.

Xerogel $\boldsymbol{HM_{ITBAF}}$. The mixture for gelation was made with 1.28 g (4.0 mmol) of **I**, 4×10^{-2} mmol of TBAF, 12 mmol of water, and 1.3 mL of THF. Mass of xerogel: 0.738 g. Yield: 102%.

Xerogel $\boldsymbol{HM_{IIAF}}$. The mixture for gelation was made with 1.29 g (3.3 mmol) of **II**, 3.27×10^{-2} mmol of NH_4F, 9.8 mmol of water, and 1.09 mL of THF. Mass of xerogel: 0.829 g. Yield: 99%.

Xerogel $\boldsymbol{HM_{IINH3}}$. The mixture for gelation was made with 1.34 g (3.3 mmol) of **II**, 13.2×10^{-2} mmol of NH_4OH, 9.9 mmol of water, and 1.13 mL of THF. Mass of xerogel: 0.862 g. Yield: 102%.

Xerogel $\boldsymbol{HM_{IINaOH}}$. The mixture for gelation was made with 1.16 g (2.9 mmol) of **II**, 11.7×10^{-2} mmol of NaOH, 8.8 mmol of water, and 0.98 mL of THF. Mass of xerogel: 0.715 g. Yield: 95%.

Xerogel $\boldsymbol{HM_{IIHCl}}$. The mixture for gelation was made with 1.48 g (3.8 mmol) of **II**, 11.25×10^{-2} mmol of HCl, 11.25 mmol of water, and 1.25 mL of THF. Mass of xerogel: 0.993 g. Yield: 103%.

Xerogel $\boldsymbol{HM_{IITBAF}}$**.** The mixture for gelation was made with 0.91 g (2.3 mmol) of **II**, 2.31×10^{-2} mmol of TBAF, 6.9 mmol of water, and 0.75 mL of THF. Mass of xerogel: 0.468 g. Yield: 79%.

Xerogel $\boldsymbol{HM_{IIIHCl}}$. The mixture for gelation was made with 0.46 g (1.3 mmol) of **III**, 4.02×10^{-2} mmol of HCl, 4.02 mmol of water, and 0.45 mL of THF. Mass of xerogel: 0.232 g. Yield: 86%.

Xerogel $\boldsymbol{HM_{IIINaOH}}$. The mixture for gelation was made with 0.42 g (1.2 mmol) of **III**, 4.8×10^{-2} mmol of NaOH, 3.63 mmol of water, and 0.40 mL of THF. Mass of xerogel: 0.177 g. Yield: 70%.

Xerogel $\boldsymbol{HM_{IVHCl}}$. The mixture for gelation was made with 0.64 g (1.7 mmol) of **IV**, 5.16×10^{-2} mmol of HCl, 5.16 mmol of water, and 0.57 mL of THF. Mass of xerogel: 0.310 g. Yield: 76%.

Xerogel $\boldsymbol{HM_{IVNaOH}}$. The mixture for gelation was made with 0.55 g (1.5 mmol) of **IV**, 5.92×10^{-2} mmol of NaOH, 4.44 mmol of water, and 0.49 mL of THF. Mass of xerogel: 0.270 g. Yield: 77%.

Xerogel $\boldsymbol{HM_{VHCl}}$. The mixture for gelation was made with 0.398 g (0.84 mmol) of **V**, 2.52×10^{-2} mmol of HCl, 2.52 mmol of water, and 0.28 mL of THF. Mass of xerogel: 0.178 g. Yield: 62%.

Xerogel $\boldsymbol{HM_{VNaOH}}$. The mixture for gelation was made with 0.607 g (1.28 mmol) of **V**, 5.12×10^{-2} mmol of NaOH, 3.84 mmol of water, and 0.43 mL of THF. Mass of xerogel: 0.243 g. Yield: 56%.

Xerogel $\boldsymbol{HM_{VIHCl}}$. The mixture for gelation was made with 0.11 g (0.22 mmol) of **VI**, 0.66×10^{-2} mmol of HCl, 0.66 mmol of water, and 0.07 mL of THF. Mass of xerogel: 0.08 g. Yield: 104%.

Xerogel $\boldsymbol{HM_{VINaOH}}$. The mixture for gelation was made with 0.20 g (0.42 mmol) of **VI**, 1.68×10^{-2} mmol of NaOH, 1.26 mmol of water, and 0.14 mL of THF. Mass of xerogel: 0.13 g. Yield: 102%.

Xerogel $\boldsymbol{HM_{VIINaOH}}$. The mixture for gelation was made with 0.54 g (1.23 mmol) of **VII**, 4.92×10^{-2} mmol of NaOH, 3.69 mmol of water, and 0.41 mL of THF. Mass of xerogel: 0.302 g. Yield: 106%.

Xerogel $\boldsymbol{HM_{VIIHCl}}$. The mixture for gelation was made with 0.51 g (1.17 mmol) of **VII**, 3.51×10^{-2} mmol of HCl, 3.51 mmol of water, and 0.39 mL of THF. Mass of xerogel: 0.322 g. Yield: 118%.

Xerogel $\boldsymbol{HM_{IIMeOH}}$. The mixture for gelation was made with 1.66 g (4.22 mmol) of **II**, 4.22×10^{-2} mmol of NH_4F, 12.66 mmol of water, and 1.41 mL of MeOH. Mass of xerogel: 1.067 g. Yield: 99%.

Xerogel $\boldsymbol{HM_{IITol.}}$. The mixture for gelation was made with 1.26 g (3.21 mmol) of **II**, 3.21×10^{-2} mmol of NH_4F, 9.63 mmol of water, and 1.07 mL of toluene. Mass of xerogel: 0.808 g. Yield: 98%.

Xerogel $\boldsymbol{HM_{IIDMF}}$. The mixture for gelation was made with 1.53 g (3.89 mmol) of **II**, 3.89×10^{-2} mmol of NH_4F, 10.68 mmol of water, and 1.30 mL of DMF. Mass of xerogel: 0.967 g. Yield: 97%.

Xerogel $\boldsymbol{HM_{IINMF}}$. The mixture for gelation was made with 0.49 g (1.24 mmol) of **II**, 1.24×10^{-2} mmol of NH_4F, 3.72 mmol of water, and 1.24 mL of NMF. Mass of xerogel: 0.309 g. Yield: 97%.

Xerogel $\boldsymbol{HM_{IIForm.}}$. The mixture for gelation was made with 0.35 g (0.88 mmol) of **II**, 0.88×10^{-2} mmol of NH_4F, 2.64 mmol of water, and 0.88 mL of formamide. Mass of xerogel: 0.220 g. Yield: 98%.

CM011180U